

Stimuli-responsive vitamin E-based micelles: Effective drug carriers with a controlled anticancer drug release

Wojciech Raj^a, Krzysztof Jerczynski^a, Mahdi Rahimi^a, Ewa Pavlova^b, Miroslav Šlouf^b, Agata Przekora^c, Joanna Pietrasik^{a,*}

^a Lodz University of Technology, Institute of Polymer and Dye Technology, Stefanowskiego 16, 90-537, Lodz, Poland

^b Institute of Macromolecular Chemistry, Czech Academy of Sciences, Heyrovského Namesti 2, 162 06, Praha 6, Czech Republic

^c Medical University of Lublin, Independent Unit of Tissue Engineering and Regenerative Medicine, Chodzki 1 Street, 20-093, Lublin, Poland

ARTICLE INFO

Keywords:

RAFT polymerization
Polymer micelles
Doxorubicin
Controlled anticancer drug release

ABSTRACT

Herein, a series of vitamin E-based TPGS-poly(2-(dimethylamino)ethyl methacrylate)-*b*-poly(3-vinyl benzaldehyde) block copolymer micelles were synthesized via reversible addition–fragmentation chain-transfer polymerization (RAFT). D- α -tocopheryl poly(ethylene glycol) 1000 succinate (TPGS) is a good candidate to overcome the big problem of multidrug resistance in cancer therapy because TPGS can inhibit permeability of glycoprotein (P-gp) resulting in restored sensitivity to chemotherapeutics. Doxorubicin (DOX) was loaded within the micelles, as an anticancer model drug, via hydrolytic amide linkage in the hydrophobic block. The DOX-loaded micelles demonstrated high potential as anticancer drug delivery systems through the release of the drug under acidic conditions, varying from pH 7.4 to 5.0. Three different micelles compositions were investigated with various ratios of hydrophilic and hydrophobic blocks (1:1, 4:3, and 4:1). The DOX-conjugated polymer with the shortest hydrophobic segment (4:1), TPGS-poly(2-(dimethylamino)ethyl methacrylate)₁₂₅-*b*-poly(3-vinyl benzaldehyde)₉₁, demonstrated excellent *in vitro* cytotoxicity with pH-responsive characteristics in comparison to free DOX. Although the higher degree of polymerization of the hydrophobic block promoted the drug loading efficiency of the micelles these compositions demonstrated lower cytotoxicity to the A549 cell line of human lung adenocarcinoma. It was concluded that the prepared pH-responsive micelles based on TPGS are promising drug carriers for anticancer drug delivery systems and could be considered to provide multi-drug resistance cancer treatments after further *in vitro* biological studies.

1. Introduction

Cancer is a leading cause of mortality worldwide [1]. Chemotherapy, radiotherapy, and surgery are the conventional approaches used frequently for the treatment of cancer [2]. Although chemotherapy is a powerful tool, the drug therapies are associated with poor bioavailability, high systemic toxicity, as well as the emergence of intrinsic multidrug resistance (MDR) [3]. MDR is still one of the main obstacles limiting successful cancer chemotherapy [4,5]. One of the best strategies to combat MDR is the use of nanomaterials that deliver the anticancer drugs efficiently to the target tumor tissue via increasing internalization and reducing permeability glycoprotein, P-gp-mediated drug efflux from cells [6,7]. As a consequence, drug delivery systems based on micelles, liposomes, dendrimers, bottlebrush polymers, magnetic nanoparticles, etc. are considered as good candidates to improve drug targeting and

efficacy [8–12].

Polymeric nanomaterials have been extensively used for cancer treatment [13]. Many kinds of polymeric nanomaterials have been developed to improve the efficacy of cancer therapeutics, such as polymer-DNA complexes (polyplexes), polymer-drug conjugates, and polymer micelles bearing hydrophobic drugs [14–17]. Among them, polymeric micelles provide a very small size range, which is critical for passive targeting to solid tumors compared to other types of polymeric drug carriers [18]. Polymeric micelles can be formed via several approaches, however, the method based on the block copolymer self-assembly is the most common. Block copolymers are usually amphiphilic macromolecules that have distinct hydrophobic and hydrophilic segments [19,20]. Despite their advantages, they have some disadvantages such as high hydrophobicity, long degradation time, long-term incompatibility with blood cells, and a tendency for

* Corresponding author.

E-mail address: joanna.pietrasik@p.lodz.pl (J. Pietrasik).

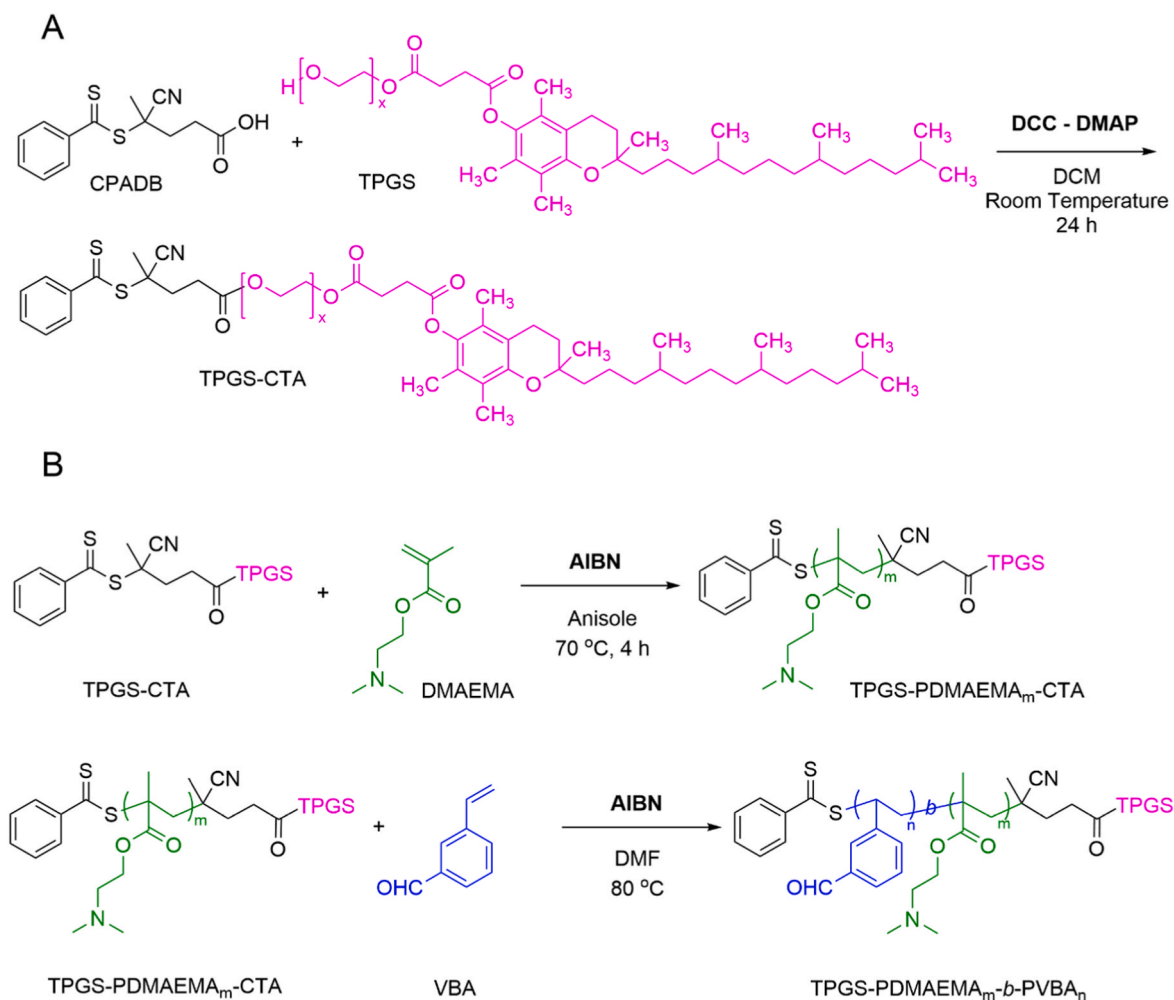


Fig. 1. Preparation of TPGS-based chain transfer agent (TPGS-CTA) (A). Sequence steps for the preparation of TPGS-PDMAEMA_m-b-PVBA_n block copolymer (B).

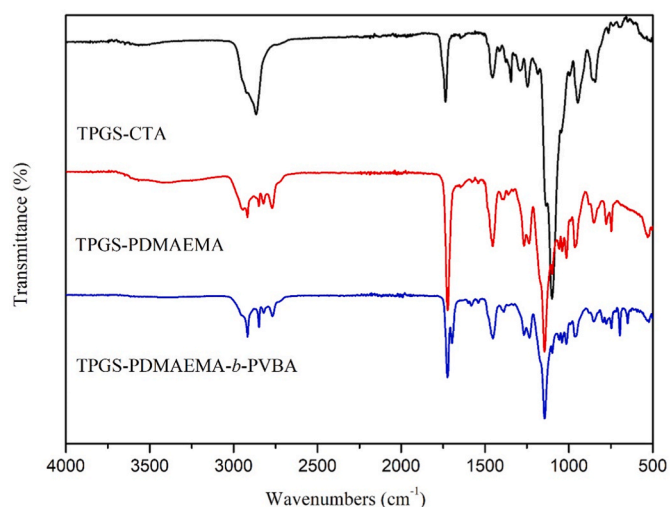


Fig. 2. FTIR spectra of TPGS-based chain transfer agent (TPGS-CTA), TPGS-PDMAEMA, and TPGS-PDMAEMA-*b*-PVBA block copolymer in the wavenumber ranges of 500–4000 cm^{-1} .

elimination by the reticuloendothelial system. Poly(ethylene glycol) (PEG) is a hydrophilic polymer that is a good candidate to enhance the hydrophilicity of the prepared polymeric carrier [21]. Furthermore, it

allows a reduction in the process of phagocytosis and opsonization of efficacy via improving the circulation time of plasma proteins in the blood [3,16]. D- α -tocopheryl poly(ethylene glycol)₁₀₀₀ succinate (TPGS) is a derivative of PEG attached to natural vitamin E via a covalent bond. Interestingly, TPGS not only has the same characteristics as PEG but is also used as an agent to overcome MDR by inhibiting P-gp, resulting in restored sensitivity to chemotherapeutics [22,23]. The U.S. Food and Drug Administration (FDA) has approved TPGS as a safe pharmaceutical adjuvant used in drug formulation [24].

Recently, several polymeric micelles based on TPGS were reported for enhancing the solubility, permeability, and stability of the formulated drugs [25–28]. In this research, a series of block copolymers were synthesized via reversible addition-fragmentation chain-transfer (RAFT) polymerization using a TPGS-based chain transfer agent (synthesized for the first time in this study) for the delivery of DOX as a model hydrophobic anticancer drug. DOX was conjugated to the micelles through imine covalent bonds which demonstrated a controlled DOX release via acidic hydrolysis under cancerous conditions. Both healthy and cancerous cells lines were treated with bare micelles and DOX-conjugated micelles, and it was observed that the bare micelles showed no significant toxic effect on human normal fibroblast (BJ cell line), while DOX-conjugated micelles showed high cytotoxic effects on human lung adenocarcinoma cells (A549 cell line). Although the MDR effect of TPGS was not investigated in this study, based on the previous reports, it was anticipated such types of micelles could be not only good candidates as drug delivery systems but also to overcome the MDR effect, evade the reticuloendothelial system (RES), and prolong the

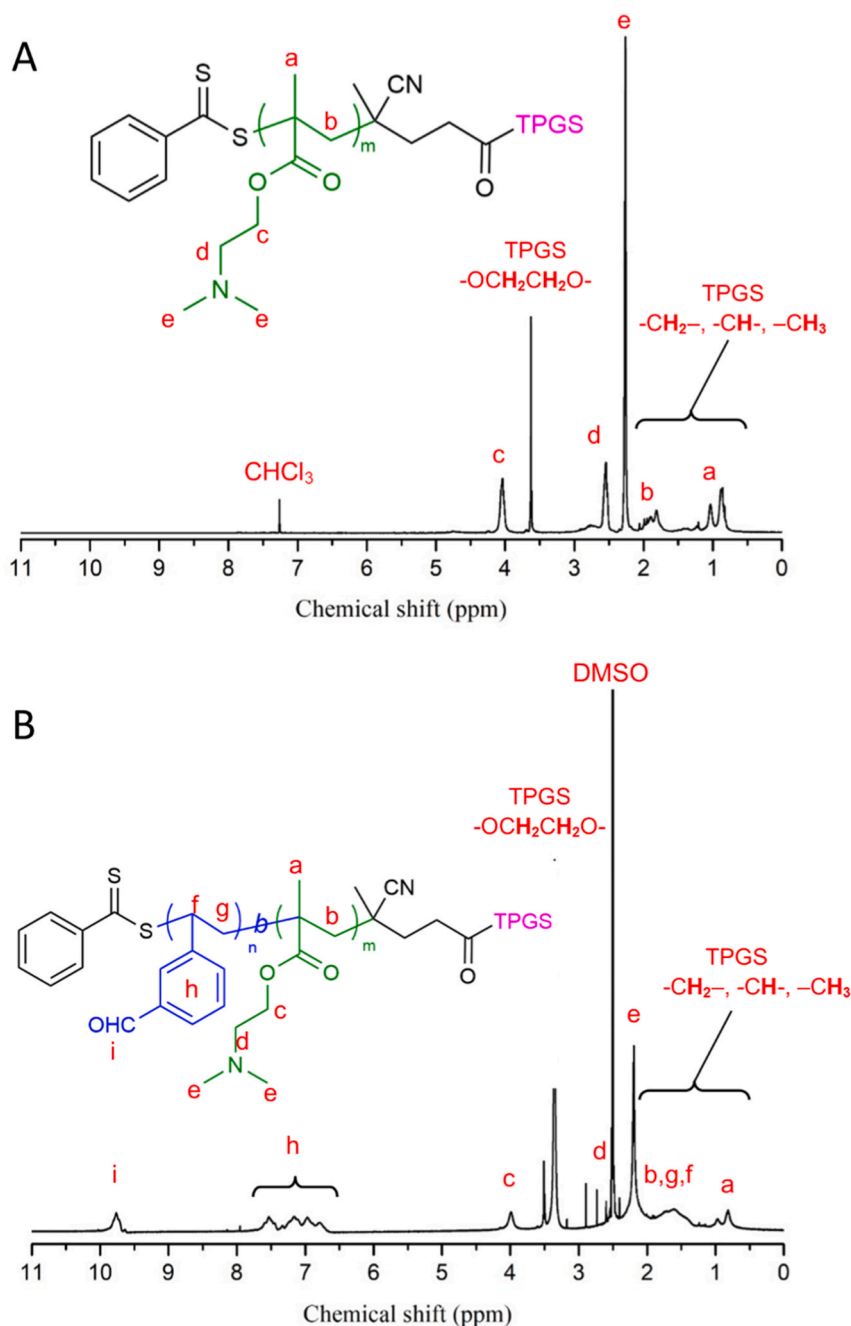


Fig. 3. ¹H NMR spectra of TPGS-PDMAEMA_m in CDCl₃ (A) and TPGS-PDMAEMA_m-b-PVBA_n in DMSO-*d*₆ (B).

micelle circulation time in the blood.

2. Experimental section

2.1. Materials

D- α -tocopherol poly(ethylene glycol) 1000 succinate (TPGS, Bio-Xtra), 4-cyano-4-(phenylcarbonothioylthio)pentanoic acid (CPADB), 4-(dimethylamino)pyridine (DMAP, $\geq 99.0\%$), N,N'-dicyclohexylcarbodiimide (DCC, 99%), 2,2'-azobis(2-methylpropanitrile) (AIBN, 98%), phosphate-buffered saline tablet (PBS), 3-vinyl benzaldehyde (VBA, 97%) were purchased from Sigma Aldrich and used as received. Doxorubicin hydrochloride (DOX.HCl, 95%) was purchased from ABCR Gute Chemie. 2-(Dimethylamino)ethyl methacrylate (DMAEMA, 98%)

received from Sigma Aldrich, was purified by distillation under reduced pressure. All solvents including, dichloromethane (DCM), methanol, diethyl ether, n-hexane, N,N-dimethylformamide (DMF) were purchased from Pure POCH and used without further purifications. Cell culture media (EMEM and F-12K) and cell lines (BJ and A549) were purchased from ATCC-LGC Standards. Fetal bovine serum (FBS) was bought from Pan-Biotech. Other cell culture reagents (penicillin, streptomycin, phosphate buffered saline, trypsin-EDTA solution) were received from Sigma-Aldrich Chemicals.

2.2. Instrumentation

The average molecular weights of synthesized polymers and their dispersities (\bar{M}_w/\bar{M}_n) were determined using a gel permeation

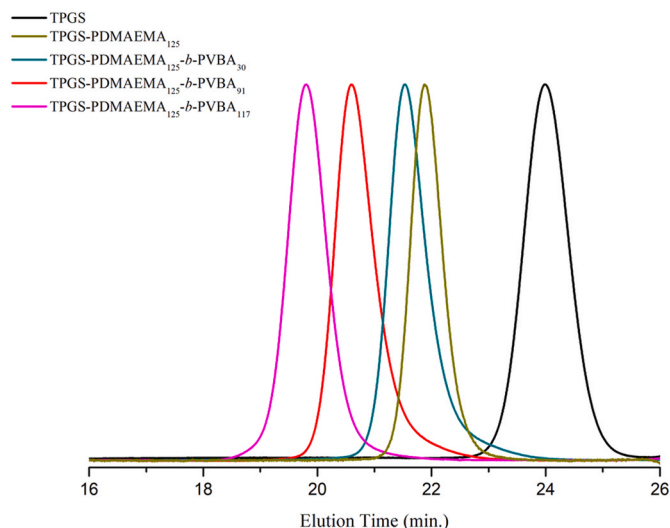


Fig. 4. GPC traces of TPGS, TPGS-PDMAEMA₁₂₅, TPGS-PDMAEMA₁₂₅-b-PVBA₃₀, TPGS-PDMAEMA₁₂₅-b-PVBA₉₁, and TPGS-PDMAEMA₁₂₅-b-PVBA₁₁₇.

Table 1
GPC and ¹H NMR characterization of TPGS-PDMAEMA_m-b-PVBA_n.

Sample	Copolymer composition (DP) ^a		M_n NMR ^a	M_n ^b	\bar{D} ^b
	PDMAEMA	PVBA			
TPGS	-	-	1,513	1,900	1.17
TPGS-PDMAEMA ₁₂₅	125	-	21,400	21,200	1.18
TPGS-PDMAEMA ₁₂₅ -b-PVBA ₃₀	125	30	25,300	25,400	1.11
TPGS-PDMAEMA ₁₂₅ -b-PVBA ₉₁	125	91	33,400	29,500	1.10
TPGS-PDMAEMA ₁₂₅ -b-PVBA ₁₁₇	125	117	36,900	32,200	1.15

^a Molecular weight and degree of polymerization based on monomer conversion calculated from ¹H NMR spectroscopy results.

^b M_n and \bar{D} determined by GPC using linear PMMA and PS standards in DMF, respectively.

chromatography (GPC) instrument, (Wyatt, Dernbach, Germany) equipped with two Perfect Separation Solutions (PSS) columns and one guard column (GRAM Linear (10 μ m, M_n between 800 and 1,000,000 Da), differential refractometer (RI) and light scattering (LS) detectors. DMF containing 50 mmol LiBr was used as eluent at a flow rate of 1 mL/min. Polystyrene (M_n between 682 and 2,520,000 Da) and poly(methyl methacrylate) standards (M_n between 602 and 2,200,000 Da) were applied. The chemical structure of the synthesized compounds and monomer conversion during the polymerization was determined by proton Nuclear Magnetic Resonance (¹H NMR). The ¹H NMR spectra were recorded on a Bruker Avance DPX 250 MHz instrument using CDCl₃ and DMSO-*d*₆ as the solvents. The average hydrodynamic diameters of the micelles were determined based on dynamic light scattering (DLS) measurements, that were performed on the Zetasizer Nano ZS90 analyzer. The concentration of polymer samples in methanol was 2 mg/mL, at 20 °C. The critical micelle concentration (CMC) was determined at room temperature using a Thermo Scientific Evolution 220 UV-Vis spectrophotometer with 1 nm resolution in the range of 200–400 nm. Pyrene was applied as a fluorescence probe. UV-Vis spectra were recorded at a constant pyrene concentration and varied polymer concentration. Graphs of intensity ratio from pyrene spectra (I_{333}/I_{318}) as a function of concentration logarithm (log(c)) were plotted, then the CMC value was calculated from the cross-over point. The same instrument was used for the analysis of DOX concentration, loaded and released from micelles at room temperature. The chemical

structure of synthesized copolymers was analyzed by Fourier transform infrared spectroscopy (FTIR) using an FTIR Nicolet 6700 spectrophotometer and OMNIC 3.2 software (Thermo Scientific Products: Riviera Beach, FL, USA). The measurements were conducted in the mid-infrared region of 4000-650 cm⁻¹ with 64 scans. An ATR accessory equipped with a single reflection diamond ATR crystal on ZnSe plate was used for all the analyses. TEM microscope Tecnai G2 Spirit Twin 12 (FEI, Brno, Czech Republic) equipped with a cryo-attachment (Gatan, CA, USA) was employed for direct visualization of the nanoparticles using two independent sample preparation techniques: fast drying (followed by standard TEM imaging) and fast freezing (followed by cryogenic TEM or cryo-TEM). The fast-dried samples for the standard TEM were prepared by dropping 2 μ L of sample solution onto a standard carbon coated copper TEM grid and leaving the droplet to evaporate for 1 min at ambient temperature. Then the excess of the solvent was removed by touching the bottom of the grid with a small stripe of filter paper. The dried sample was left to equilibrate at ambient temperature for >1 h, prior to being inserted in the TEM microscope and observed at the accelerating voltage of 120 kV. The samples for the cryo-TEM were prepared and observed as follows: 3 μ L of the sample solution were dropped onto an electron microscopy grid covered with a holey carbon supporting film (Electron Microscopy Science), which was hydrophilized just before the experiment by means of glow discharge (Expanded Plasma Cleaner, Harrick Plasma, USA). The excess of the solution was removed by blotting (Whatman no. 1 filter paper) for 1 s and the grid was plunged into liquid ethane held at -181 °C. The frozen sample was immediately inserted in the cryo-holder, transferred into the TEM microscope and observed at -173 °C using bright field imaging at the accelerating voltage of 120 kV.

2.3. Preparation of block copolymer micelles

2.3.1. Synthesis of TPGS-based chain transfer agent (TPGS-CTA)

DCC (0.78 g, 3.80 mmol) was dissolved in DCM (10 mL) in a round bottom flask, then TPGS (5.00 g, 3.31 mmol) and the solution of CPADB (0.92 g, 3.31 mmol in 20 mL DCM) were added to the flask. The reaction mixture was cooled to 0 °C in an ice bath and a solution of DMAP (0.44 g, 3.64 mmol in 10 mL DCM) was added dropwise. The reaction was allowed to progress under argon atmosphere in a dark environment at room temperature for 24 h. Then, the solvent was evaporated and obtained crude product was dissolved in methanol. The resulting solution was precipitated twice in diethyl ether and once in n-hexane. The product was stored under an argon atmosphere in the fridge. The calculated yield of the reaction was 87%, based on ¹H NMR spectra.

2.3.2. Preparation of TPGS-poly(2-(dimethylamino)ethyl methacrylate), TPGS-PDMAEMA_m-CTA, by RAFT polymerization

DMAEMA (10.00 mL, 29.67 mmol), TPGS-CTA (0.42 g, 0.119 mmol), AIBN (0.0039 g, 0.012 mmol), and anisole (17.00 mL) were added to a 50 mL Schlenk flask and the resulting solution was degassed by argon for 45 min prior to the flask being immersed in an oil bath at 70 °C for 4 h. The obtained polymer was re-dissolved in THF and reprecipitated in cold n-hexane three times. The final product was dried under vacuum conditions at 25 °C and 40 mbar pressure for 24 h. The obtained TPGS-PDMAEMA_m was kept under an argon atmosphere in the fridge.

2.3.3. Preparation of TPGS-poly(2-(dimethylamino)ethyl methacrylate)-b-poly(3-vinyl benzaldehyde), (TPGS-PDMAEMA_m-b-PVBA_n), by RAFT polymerization

VBA (1.49 g, 6.422 mmol), TPGS-PDMAEMA (0.6125 g, 0.032 mmol), AIBN (0.9 mg, 0.003 mmol) and DMF (4.00 mL) were added to a 50 mL Schlenk flask. The solution was degassed by argon for 45 min and then the flask was immersed in an oil bath at 80 °C for different reaction times (4, 6, and 12 h) to obtain the diblock-copolymers. The obtained polymers were diluted with methanol and purified by dialysis in methanol (Regenerated Cellulose Dialysis Membrane ZelluTransRoth MWCO

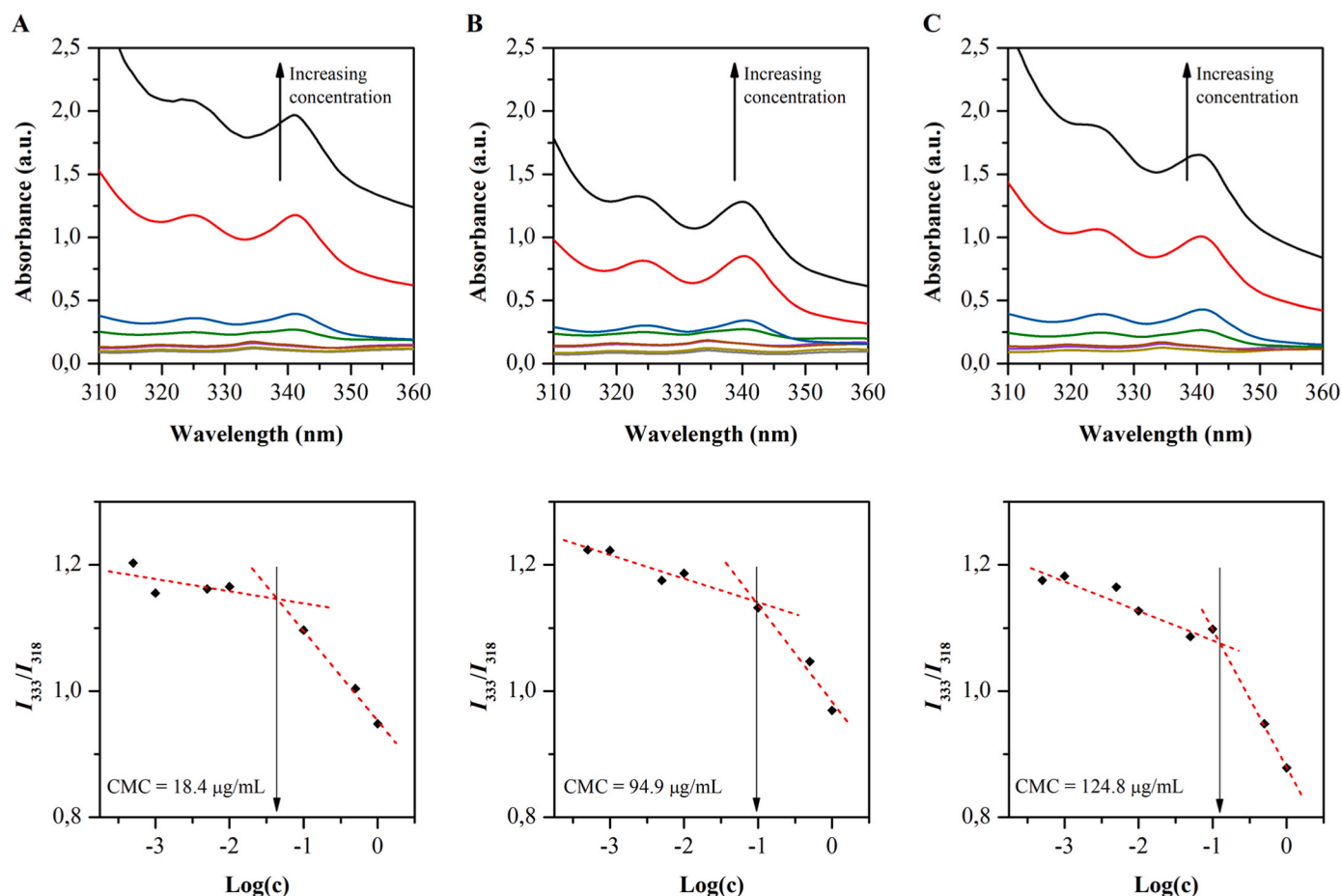


Fig. 5. Fluorescence excitation spectra of pyrene (7.5×10^{-6} mol/L) in TPGS-PDMAEMA₁₂₅-b-PVBA₃₀ (A), TPGS-PDMAEMA₁₂₅-b-PVBA₉₁ (B), and TPGS-PDMAEMA₁₂₅-b-PVBA₁₁₇ (C) polymer solutions (5.0×10^{-4} ÷ 1.0 mg/mL in PBS solution) at room temperature (Upper graphs). Plots of intensity ratio obtained based on pyrene spectra (I_{333}/I_{318}) in PBS solution versus copolymer concentrations; TPGS-PDMAEMA₁₂₅-b-PVBA₃₀ (A), TPGS-PDMAEMA₁₂₅-b-PVBA₉₁ (B), and TPGS-PDMAEMA₁₂₅-b-PVBA₁₁₇ (C) at room temperature (Lower graphs).

3.5 kDa). The final products were dried in a vacuum oven at 25 °C, and 40 mbar for 24 h. The obtained block-copolymers were kept under an argon atmosphere in the fridge.

2.4. Critical micelle concentration (CMC)

The CMCs of the polymers was determined by UV-Vis spectrophotometry in PBS solution using pyrene as a fluorescence probe [29]. In brief, aliquots of pyrene in acetone (5 μL) were added to polymer solutions with varied concentrations (5.0×10^{-4} ÷ 1.0 mg/mL in PBS), next acetone was allowed to evaporate, and samples were left to equilibrate. Final pyrene concentration in the samples was 7.5×10^{-6} mol/L. The CMC was estimated from pyrene fluorescence spectra as the cross point by extrapolating the intensity ratio I_{338}/I_{333} as a function of the concentration logarithm (log(c)).

2.5. Preparation of TPGS-PDMAEMA_m-b-PVBA_n-conjugated DOX micelles

TPGS-PDMAEMA_m-b-PVBA_n block copolymer (150 mg), DOX.HCl (150 mg) and TEA (150 μL) were dissolved in 20 mL DMSO (20 mL) in a round bottom flask. The reaction was carried out under argon atmosphere and in a dark environment at room temperature for 72 h. The obtained dark red solution was dialyzed (MWCO 3.5 kDa) against phosphate-buffered saline (PBS, pH ~ 7.4) for 24 h to remove unreacted DOX. The dried polymer was obtained after lyophilization. To calculate the amount of drug in TPGS-PDMAEMA_m-b-PVBA_n-DOX (DOX-Micelle)

10 mg of the block copolymer was dissolved into the 5 mL of PBS solution and stirred for 2 h. Then, the absorbance of the solution was measured by a UV-Vis spectrophotometer. The drug content in the block copolymer was calculated according to the following formula [30].

$$\text{Drug Loading Efficiency(\%)} = \frac{\text{mass of DOX in the DOX - Micelle}}{\text{mass of DOX - Micelle}} \times 100$$

2.6. In vitro acid-triggered drugs release

A drug release study was performed for the synthesized pH-responsive micelles at two pH values, 5.0 (cancerous endosomal condition) and 7.4 (physiological condition). In order to accomplish this, 45 mg of TPGS-PDMAEMA_m-b-PVBA_n-DOX was dissolved in 20 mL PBS solution with the mentioned pH values, then the solutions were poured into dialysis bags (MWCO 3.5 kDa) and the dialysis bags were immersed into 130 mL PBS solution with the same pH values. In order to evaluate the DOX release, 2 mL PBS solution was taken out at predetermined time intervals, and the absorbance was analyzed at 480 nm by UV-Vis spectrophotometer. The release study was performed in duplicate, and the average value was reported, according to the following equation.

$$\text{Drug release(\%)} = \frac{\text{Amount of DOX release}}{\text{Amount of DOX on the DOX - Micelle}} \times 100$$

2.7. In vitro cytotoxicity assay

Cytotoxicity tests were conducted using the human lung

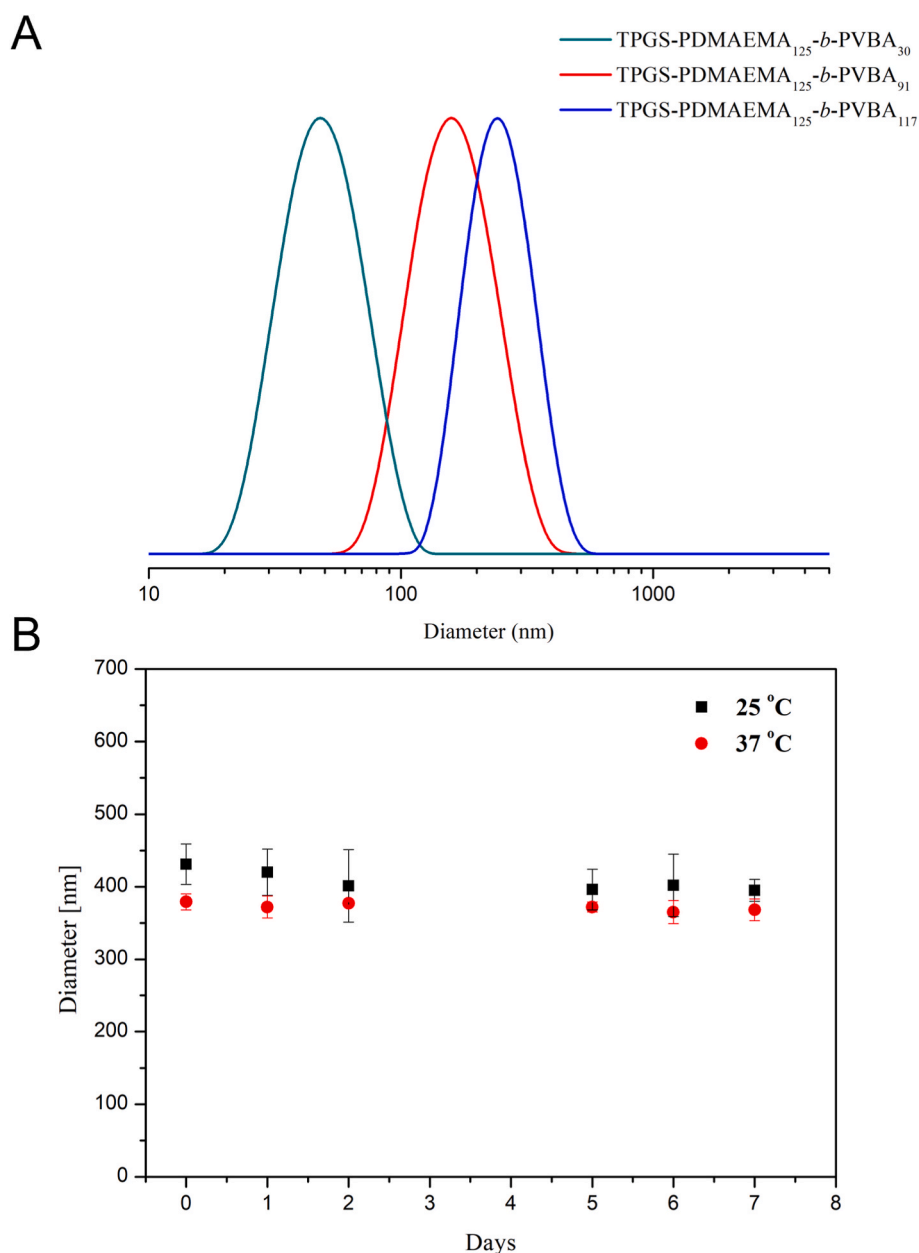


Fig. 6. (A) Determination of the hydrodynamic diameter of block copolymers micelles TPGS-PDMAEMA_m-*b*-PVBA_n at the concentration of 2 mg/mL in methanol by DLS. (B) The stability of TPGS-PDMAEMA₁₂₅-*b*-PVBA₁₁₇ in an aqueous solution at two different temperatures (25 and 37 °C).

adenocarcinoma cell line (A549, ATCC®, CCL-185TM) and a normal human skin fibroblast cell line (BJ, ATCC®, CRL-2522TM). The cells were cultured at 37 °C, in a humidified atmosphere, with 5% CO₂, 95% air, in the recommended ATCC culture medium (EMEM and F-12K for BJ cells and A549 cells, respectively). The culture media were supplemented with 10% fetal bovine serum (FBS), 100 U/mL penicillin, and 100 µg/mL streptomycin. The cells were seeded in 96-multiwell plates at a concentration of 1×10^4 cells/well, with a volume of 100 µL of the culture medium in each well. The plates were incubated for 24 h and then the culture media were replaced with 100 µL of different concentrations of the micelles solutions, or free DOX prepared in culture media containing 2% FBS. Stock solutions of the compounds and reference drug (DOX) were prepared in the phosphate buffered saline (PBS). Free DOX was tested at following concentrations: 200, 100, 50, 25, 12.5, 6.25, 3.125, 1.562, 0.781, and 0.390 µg/mL. All blank micelles and DOX-conjugated micelles were tested using the following concentrations: 2000, 1000, 500, 250, 125, 62.5, 31.25, 15.62, 7.81, and 3.90 µg/

mL. The values of loaded DOX concentrations in DOX-conjugated micelles were not the same due to the different drug loading efficiency. Cells maintained in fresh culture medium with 2% FBS served as a negative control of cytotoxicity (cell viability considered as 100%).

BJ and A549 cells were exposed to the investigated compounds for 24 h, then their viability was assessed by colorimetric MTT assay according to the procedure described previously [31]. Three independent experiments ($n = 3$) were carried out in quadruplicate. The IC₅₀ values, which indicate the concentration of the tested compound able to reduce cell viability by 50%, were calculated using GraphPad Prism 5, Version 5.03 Software. Based on the obtained IC₅₀ values for both normal BJ cells and cancer A549 cells, the *in vitro* selectivity/safety index (SI) was calculated based on the formula: $SI = IC_{50} \text{ normal cells} / IC_{50} \text{ cancer cells}$. Anticancer agents may be considered to be safe if their SI value is higher than 1.

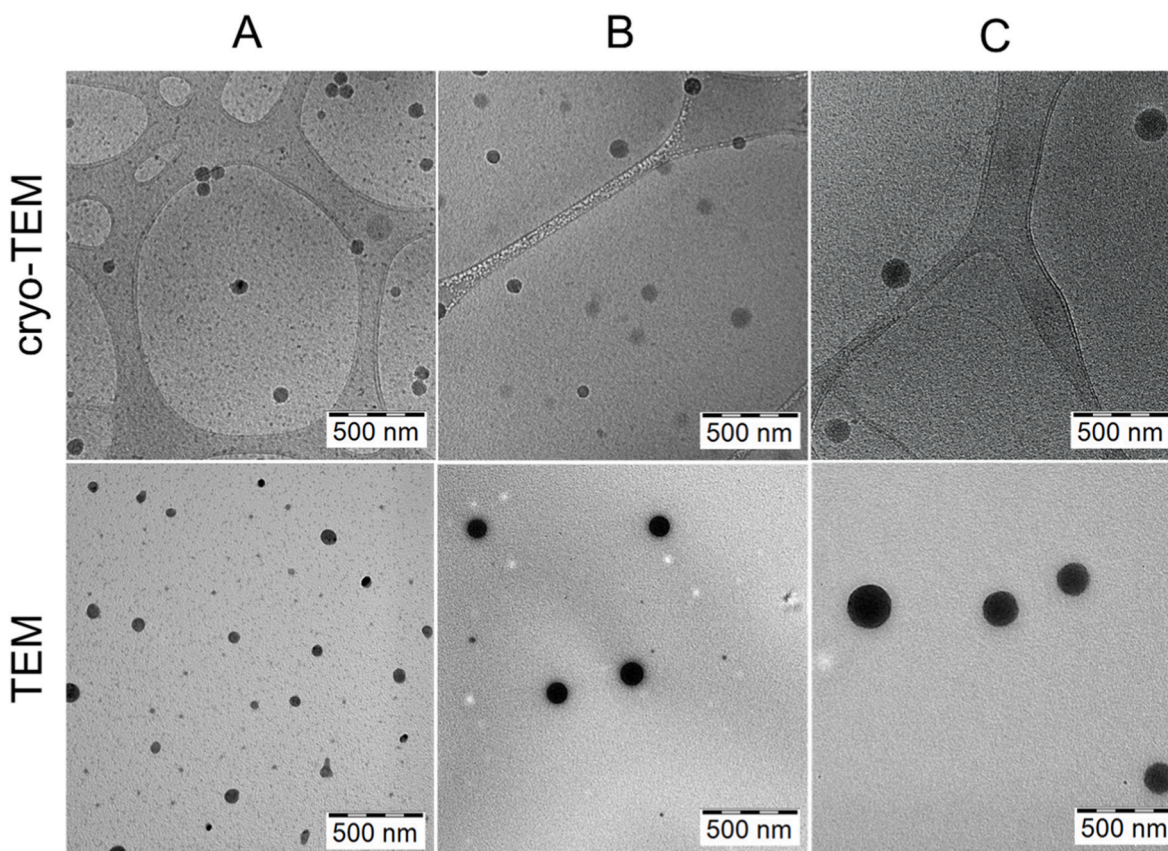


Fig. 7. Cryo-TEM and TEM micrographs of TPGS-PDMAEMA₁₂₅-b-PVBA₃₀ (A), TPGS-PDMAEMA₁₂₅-b-PVBA₉₁ (B), and TPGS-PDMAEMA₁₂₅-b-PVBA₁₁₇ (C) micelles.

Table 2
TPGS-PDMAEMA-*b*-PVBA based micelles characterization.

Sample	DOX content (%)		CMC [$\mu\text{g}/\text{mL}$] ^a	Diameter [nm], PDI ^b	Diameter [nm], PDI ^c
	UV-Vis	¹ H NMR			
TPGS- PDMAEMA ₁₂₅ - <i>b</i> - PVBA ₃₀	-	-	18.4	51 ± 1, 0.125	85 ± 3, 0.252
TPGS- PDMAEMA ₁₂₅ - <i>b</i> - PVBA ₉₁	-	-	94.9	136 ± 3, 0.227	301 ± 18, 0.199
TPGS- PDMAEMA ₁₂₅ - <i>b</i> - PVBA ₁₁₇	-	-	124.8	246 ± 10, 0.214	379 ± 36, 0.255
TPGS- (PDMAEMA ₁₂₅ - <i>b</i> - PVBA ₃₀)-DOX	9.1	9.4	-	-	381 ± 30, 0.228
TPGS- (PDMAEMA ₁₂₅ - <i>b</i> - PVBA ₉₁)-DOX	32.3	33.9	-	-	445 ± 35, 0.259
TPGS- (PDMAEMA ₁₂₅ - <i>b</i> - PVBA ₁₁₇)-DOX	41.1	43.3	-	-	466 ± 40, 0.278

^a Determined by UV-Vis in PBS solution at 25 °C.

^b Determined by DLS in methanol at 25 °C.

^c Determined by DLS in water at 37 °C.

2.8. Statistical analysis

Cell culture results were presented as mean values ± standard error of the mean (SEM). The results were analyzed for statistical significance (considered at $p < 0.05$) using an unpaired *t*-test (GraphPad Prism 8.0.0 Software). Each group of the tested compounds was compared to the

negative control.

3. Results and discussion

3.1. Preparation and characterization of TPGS-PDMAEMA_m-*b*-PVBA_n

Fig. 1 shows the synthetic steps for the preparation of TPGS-PDMAEMA_m-*b*-PVBA_n block copolymer with hydrophilic and hydrophobic domains, respectively. In the first step, CPADB as a RAFT chain transfer agent (CTA) was linked to TPGS through a coupling reaction to yield TPGS-CTA. In this regard, the carboxylic functional group of CPADB was activated with DCC (as a coupling agent)/DMAP and it was then reacted with the hydroxyl functional group of TPGS (Fig. 1A). The resulting TPGS-CTA was used as a macro-CTA for the RAFT polymerization step with AIBN as a radical source. In this study, DMAEMA was chosen as the monomer for the polymerization of the first block that would subsequently generate the hydrophilic thermo-responsive domain. RAFT polymerization of DMAEMA was performed in anisole at 70 °C to give TPGS-PDMAEMA (TPGS-CTA/AIBN/DMAEMA:1/0.1/250). After purification and isolation by precipitation into excess *n*-hexane, the chemical structure of the resulting TPGS-PDMAEMA was confirmed by FTIR and ¹H NMR spectroscopy. Then, the chain extension polymerizations of VBA monomer were done to form the second block with various degrees of polymerization that would provide the hydrophobic domains (Macro-CTA/AIBN/VBA:1/0.1/200). The final block copolymer (TPGS-PDMAEMA_m-*b*-PVBA_n) included two blocks while TPGS was attached to the hydrophilic part (Fig. 1B). In order to load DOX on the polymeric chains, TPGS-PDMAEMA_m-*b*-PVBA_n was reacted with DOX.HCl in the presence of TEA. The free amine functional group of DOX reacted with the pendant aldehyde moieties via Schiff-base reaction to generate the TPGS-PDMAEMA_m-*b*-PVBA_n-conjugated DOX micelles after dialysis of the solution in PBS. The final DOX-micelles

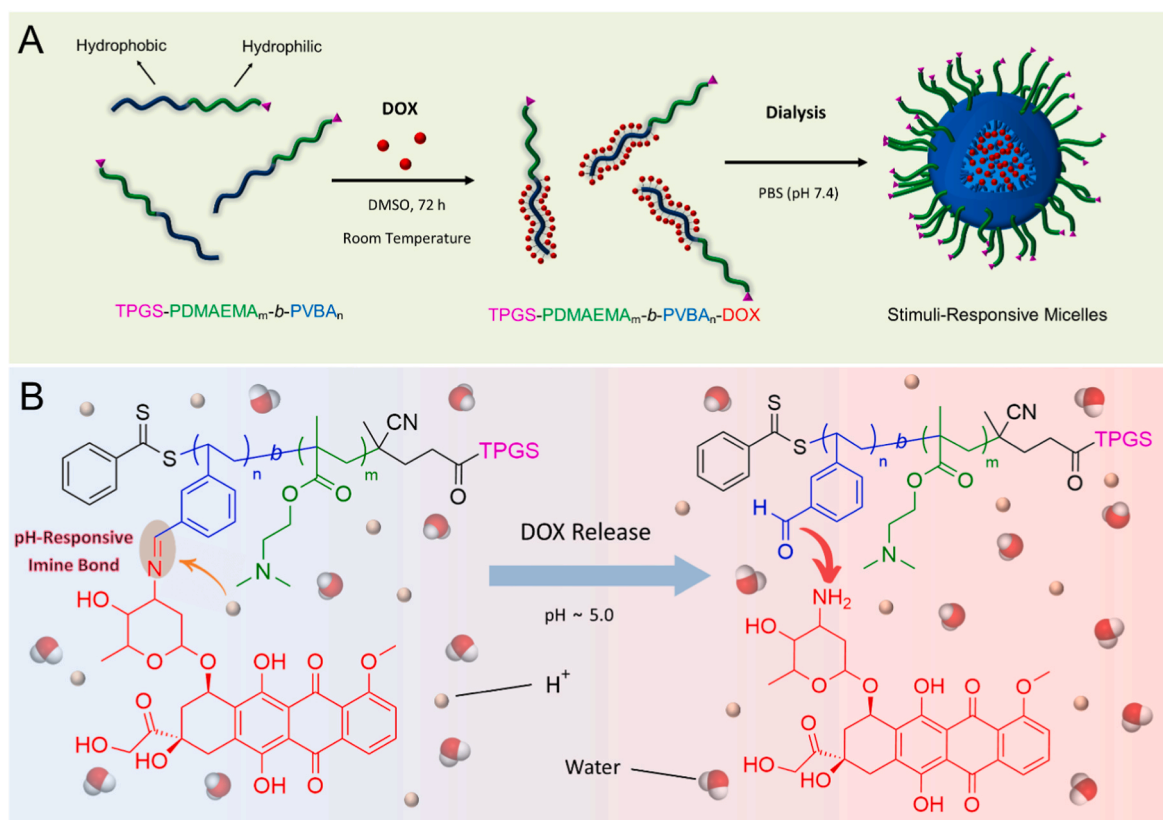


Fig. 8. Sequence steps for preparation of DOX-conjugated polymer and DOX-Micelles (A), and *in vitro* drug release under acidic condition (B).

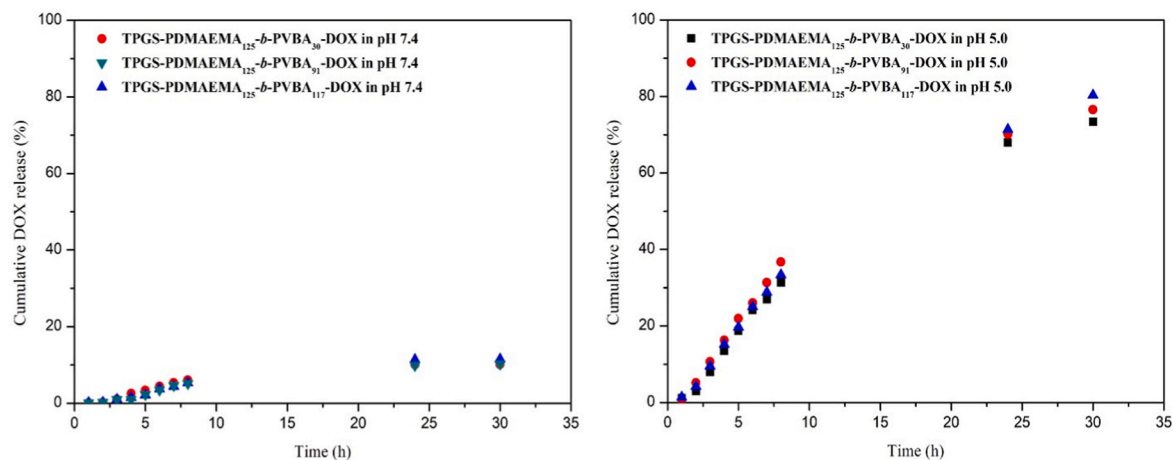


Fig. 9. *In vitro* controlled release profiles from TPGS-PDMAEMA-*b*-PVBA-conjugated DOX micelles in different pH media at 37 °C pH 7.4 and pH 5.0.

were successfully lyophilized and used for the next *in vitro* release and cytotoxicity studies.

The chemical structures of the synthesized compounds were confirmed by FTIR spectroscopy. The FTIR spectrum of the CPADB RAFT agent showed the characteristic broad bands absorption, around 3000 cm^{-1} due to the stretching vibration of carboxylic acid (-COOH). This band is almost overlapped with C-H aliphatic absorption band (2850-2950 cm^{-1}). The stretching vibrations of the carbonyl (C=O) and cyanide (CN) groups were observed around 1745 cm^{-1} and 2230 cm^{-1} , respectively. Furthermore, the characteristic bond of aromatic rings (C=C) appeared at 1420 cm^{-1} . The stretching vibrations of the C=S and C-S were observed at 1090 and 770 cm^{-1} , respectively (Fig. S1). TPGS showed four characteristic peaks including alkoxy (C-O), carbonyl

(C=O), and aliphatic methylene (CH_2) at 1100, 1715, and 2890 cm^{-1} , respectively. It also displayed a broad peak with low intensity at 3200 cm^{-1} that can be attributed to the terminal hydroxyl (O-H) bonds (Fig. S1). In the FTIR spectrum of pure TPGS-CTA, the strong absorption of a carbonyl band at 1737 cm^{-1} was observed, with slight shifting and the stretching vibration bands relating to the C=S and C-S were also observed with low intensity which confirmed the formation of TPGS-CTA. For the TPGS-PDMAEMA copolymer, the carbonyl (C=O) stretching vibration band was shifted to 1715 cm^{-1} which is different from the TPGS-CTA spectrum. The C-H stretching vibration bands appeared at the range of 2860-2940 cm^{-1} and the absorption bands at 1110 and 1250 cm^{-1} can be attributed to the C-O and C-N stretching, respectively. Almost all the signals that corresponded to the TPGS-

Table 3

Cytotoxicity of the tested micelles presented as IC₅₀ values and selectivity index (SI) determined using cancer (A549) and normal (BJ) cells (based on MTT assay performed after 24 h of exposure to tested compounds).

Tested compound	A549 cell line IC ₅₀ (μg/mL) ± SEM	BJ cell line IC ₅₀ (μg/mL) ± SEM	SI [IC ₅₀ BJ/IC ₅₀ A549]
TPGS-PDMAEMA ₁₂₅ -b-PVBA ₃₀	36.0 ± 1.1	21.6 ± 1.3	0.6
TPGS-PDMAEMA ₁₂₅ -b-PVBA ₉₁	48.0 ± 1.1	41.9 ± 1.0	0.9
TPGS-PDMAEMA ₁₂₅ -b-PVBA ₁₁₇	124.7 ± 1.2	78.6 ± 1.1	0.6
TPGS-PDMAEMA ₁₂₅ -b-PVBA ₃₀ -DOX	5.5 ± 1.3	42.6 ± 1.2	7.7
TPGS-PDMAEMA ₁₂₅ -b-PVBA ₉₁ -DOX	8.3 ± 1.4	196.0 ± 1.2	23.6
TPGS-PDMAEMA ₁₂₅ -b-PVBA ₁₁₇ -DOX	21.5 ± 1.2	171.7 ± 1.4	8.0
Free DOX	7.9 ± 1.3	36.6 ± 1.2	4.6

PDMAEMA-*b*-PVBA block copolymer were overlapped with the TPGS-PDMAEMA copolymer. Whereas, the stretching vibration bands of the aldehyde (CHO) pending groups could be detected at 2690 and 1685 cm⁻¹ confirming the formation of PVBA in the second block [32]. Consequently, all FTIR results validated that the block copolymer was successfully synthesized (Fig. 2).

The chemical structure of the synthesized (co)polymers was confirmed by ¹H NMR spectroscopy. Firstly, the resonance signals of initial reagents (CPADB and TPGS) were characterized to find their main chemical shifts. As seen in Fig. S2, the ¹H NMR spectrum of the CPADB RAFT agent showed characteristic resonance signals of protons related to C-H aromatic groups at δ = 7.4–7.8 ppm and carboxylic acid (-COOH) at δ = 12.30 ppm. The characteristic resonance signals of protons related to methyl (-CH₃) and methylene groups (-CH₂-CH₂-) also appeared at δ = 1.74 ppm and δ = 2.34 ppm, respectively. The ¹H NMR spectrum of TPGS showed that the resonance signals of protons related to the terminal hydroxyl group (-OH) and methylene groups (-CH₂CH₂-) appeared at δ = 4.58 and 4.18 ppm, respectively. The characteristic peaks of methylene groups and methyl group (-CH-, -CH₂-, and -CH₃) relating to the vitamin E section were observed at the chemical shift range of δ = 0.8–2.4 ppm (Fig. S3). After coupling CPADB and TPGS, it was expected that the resonance signals of protons related to the terminal hydroxyl group in TPGS (δ = 4.58 ppm) and carboxylic acid in CPADB (δ = 12.30 ppm) should disappear, whereas, other resonance signals of protons appeared at the same chemical shifts with only slight shifting. As a consequence, the ¹H NMR spectrum of pure TPGS-CTA confirmed that it was successfully synthesized (Fig. S4). DMAEMA monomer was polymerized by RAFT polymerization to yield TPGS-PDMAEMA-CTA and the protons of the monomer and the protons of the methyl and methylene groups were identified by ¹H NMR spectroscopy. The resonance signals of protons appeared at δ = 2.25 ppm for methyl groups associated with amine (e), δ = 1.70–2.10, 2.55, and 4.05 ppm for methylene (b, d, and c), and δ = 0.80–1.20 ppm for methyl groups (a). Additionally, the main signals attributed to the methylene groups of ethylene glycol repeating units in TPGS and methyl and methylene groups of vitamin E section were observed at δ = 2.30 and 0.80–2.00 ppm, respectively (Fig. 3A). After chain extending the TPGS-PDMAEMA-CTA (as a macro-RAFT agent) with VBA monomer to afford TPGS-PDMAEMA-*b*-PVBA, signals of protons for methylene groups (g and f) related to the PVBA were overlapped with the signals of TPGS-PDMAEMA-CTA (in the broad range, 1.45–2.00 ppm). However, the PVBA block showed new resonance signals of protons attributed to the C-H aromatic and aldehyde (-CHO) which could be assigned at δ = 6.60–7.70 and 9.77 ppm, respectively (Fig. 3B).

¹H NMR spectroscopy was used for the calculation of monomer conversion and determination of molecular weight (M_n NMR) and degree

of polymerization (DP) of the synthesized copolymer. Furthermore, the GPC analysis was performed for the determination of number average molecular weight (M_n), and dispersity (\mathcal{D}). Firstly, TPGS was analyzed with GPC to measure the average molecular weight and dispersity which showed a unimodal and symmetric peak with $M_n = 1,900$ g/mol and low dispersity ($\mathcal{D} = 1.17$). The DP value for TPGS-PDMAEMA homopolymer was calculated to be ~125. The GPC trace also demonstrated a well-defined structure of the homopolymer with a number average molecular weight of $M_n = 21,200$ g/mol which was very similar to the ¹H NMR molecular mass, M_n NMR = 21,400 g/mol. As molecular weight was changed significantly, the GPC peak shifted to lower elution time (higher molecular weight) which confirmed the successful polymerization of TPGS-PDMAEMA₁₂₅ (Fig. 4). The resulting polymer was chain extended with different lengths of PVBA blocks (DP ~ 30, 91, and 117). The final copolymer molecular weight was calculated based on ¹H NMR and GPC and is also reported. Furthermore, the low dispersity values for all samples revealed that all block copolymers were synthesized in a controlled manner. All ¹H NMR and GPC results are summarized in Table 1.

3.2. Preparation and characterization of TPGS-PDMAEMA_m-*b*-PVBA_n micelles

TPGS-PDMAEMA_m-*b*-PVBA_n micelles and their corresponding DOX conjugated micelles were prepared using the dialysis method. For characterization of the micelles their size as well as CMC needed for micelles formation were determined using DLS and TEM analyses. CMC was measured to find an optimized concentration in which the micelles are stable. The hydrodynamic size diameters of the micelles were recorded by DLS techniques before and after conjugating DOX. Furthermore, TEM analysis was performed to confirm the successful synthesis of the micelles. All obtained results are discussed in detail in the following section.

The fluorescence emission spectra of pyrene were used to determine the micellization potential of the TPGS-PDMAEMA_m-*b*-PVBA_n in PBS solution. Fig. 5A shows the fluorescence spectra of pyrene in polymer solutions with different concentrations. The intensity ratio of I_{333} to I_{318} in the emission spectra of pyrene is rather sensitive to the polarity of the external medium. During micelle formation, the pyrene molecules are transferred from a hydrophilic microenvironment to a hydrophobic one, leading to a significant decrease of I_{333}/I_{318} . Fig. 5B illustrates the change of I_{333}/I_{318} as a function of the concentration at 25 °C in the PBS solution of TPGS-PDMAEMA_m-*b*-PVBA_n. It can be observed that I_{333}/I_{318} ratios demonstrate a sudden decrease of I_{333}/I_{318} values at around 18.4, 94.9, and 127.8 μg/mL, respectively. Pyrene molecules were present in an aqueous environment at low concentrations due to the existence of separated polymer chains. Because the polymer chains did not interact with each other at a low concentration, no micelles were formed and as a result, the value of I_{333}/I_{318} was only measured with high intensity. On the other hand, by increasing the polymer concentration, it started to self-assemble into micelles, including pyrene molecules into the more hydrophobic core of the micelles, and the ratio of I_{333}/I_{318} decreased dramatically. The CMC value can be estimated from the cross-over point, and they are 18.4, 94.9, and 124.8 μg/mL for TPGS-PDMAEMA₁₂₅-*b*-PVBA₃₀, TPGS-PDMAEMA₁₂₅-*b*-PVBA₉₁, and TPGS-PDMAEMA₁₂₅-*b*-PVBA₁₁₇, respectively. From a clinical standpoint, the relatively low CMC means that the structure of the micelles can remain stable after injection of micelles into a human body; even though they are diluted by blood [33,34]. Cumulatively, the low-value CMC of TPGS-PDMAEMA₁₂₅-*b*-PVBA₁₁₇ suggests that it forms a stable micelle in an aqueous solution, which is important for the robust encapsulation of drugs.

Dynamic light scattering (DLS) measurements were conducted, using methanol and water as a solvents, in order to investigate the size of the micelles in solution (Fig. 6A). As seen in the graph, the hydrodynamic diameters of prepared TPGS-PDMAEMA₁₂₅-*b*-PVBA₃₀, TPGS-PDMAEMA₁₂₅-*b*-PVBA₉₁, and TPGS-PDMAEMA₁₂₅-*b*-PVBA₁₁₇ micelles

were 85 ± 3 nm, 301 ± 18 nm, and 379 ± 36 nm, respectively. The micelles comprising-conjugated DOX were also analyzed by DLS and in this case, the hydrodynamic diameters were around 381 ± 30 nm, 445 ± 35 nm, and 466 ± 40 nm, respectively, due to the presence of the entrapped hydrophobic drug inside the formed micelles.

According to the recent literature, the suitable size for the accumulation of particles in the tumor tissue via the Enhanced Permeability and Retention (EPR) effect for cancer therapy is around 50–200 nm [35]. To achieve a better EPR effect and accumulation of particles in the tumor tissue, the aqueous stability of the prepared micelles should be also evaluated. Therefore, the serum stability of prepared micelles was tested at different temperatures. As an example, TPGS-PDMAEMA₁₂₅-*b*-PVBA₁₁₇ was chosen for the stability evaluation by DLS at two different temperatures: 25 °C (room temperature) and 37 °C (physiological temperature) (Fig. 6B). In this regard, the prepared micelles were incubated at the mentioned temperatures for a predetermined time and then the hydrodynamic size was measured. The hydrodynamic size did not change significantly after incubation of the micelle for one week. Besides, micelles at higher temperatures have smaller sizes, because the PDMAEMA block is a temperature-responsive polymer, which demonstrates a low critical solution temperature (LCST) behavior. Therefore, it can be concluded that the prepared micelles demonstrate acceptable serum stability in the aqueous solution and show thermo-responsive properties which can help for bursting drug release.

The micelles were also visualized by TEM (Fig. 7). Each sample was prepared and observed in two independent ways: by fast freezing followed by cryo-TEM (Fig. 7, upper row) and by fast drying followed by standard TEM (Fig. 7, lower row). The cryo-TEM and standard TEM results were in good agreement, which indicated reliability and reproducibility of microscopic analyses. On the other hand, the average particle diameters on TEM micrographs (ranging from ca 100–250 nm) were slightly lower than the corresponding hydrodynamic diameters from DLS (Fig. 6). This could be attributed to nanoparticle aggregation, which increased the particle average size in DLS (and which was observed also on TEM micrographs that are not shown for the sake of brevity). In any case, the non-aggregated micelles displayed in Fig. 7 showed well-defined spherical shapes and their average size increased with the length of the polymer chains; this was in perfect agreement with DLS measurements.

3.3. *In vitro* drug loading and drug release

The drug loading conjugation efficiency was calculated based on ¹H NMR and UV–Vis spectroscopy (Table 2). The obtained results from both methods were consistent and the amount of conjugated DOX in the prepared micelles (TPGS-PDMAEMA₁₂₅-*b*-PVBA₃₀, TPGS-PDMAEMA₁₂₅-*b*-PVBA₉₁, and TPGS-PDMAEMA₁₂₅-*b*-PVBA₁₁₇) were found to be as high as 9.1%, 32.3%, and 41.1% w/w (based on UV–Vis spectroscopy). The values of drug loading efficiency for loaded drug micelles were comparable, or better, than those reported in the literature for prodrug micelles, less than 10% w/w [36]. Because DOX was conjugated to the hydrophobic side of the chains with aldehyde pending groups through the Schiff-base reaction, by increasing the length (degree of polymerization) of the hydrophobic part, the content of loaded drug also increased (Fig. 8A). All data obtained from drug loading are acceptable for drug delivery systems, because high drug payload can be very effective for delivery of DOX and hence can improve therapeutic efficacy in the treatment of cancer. For the drug-releasing study, the DOX-conjugated micelles were suspended in PBS solutions with pH values of 7.4 and 5.0, i.e. that corresponds to physiological and cancerous tissue conditions, respectively. DOX was conjugated to the polymer chains in the micelles via imine bonds which are liable under a mild acidic condition (pH 5.0), whereas this bond is quite stable under physiological conditions (pH 7.4). As a consequence, it was expected that DOX should be released in a controlled way under acidic conditions in comparison to the neutral condition. The proposed drug release

mechanism of DOX-conjugated micelles was illustrated in Fig. 8B. The DOX release profile revealed that all three DOX-conjugated micelles showed low drug cumulative release of less than 18% at pH 7.4. While, all formulations demonstrated a burst and controlled release of almost more than 80% at pH 5.0 (Fig. 9). Another point that could be found out from the release profile is increased DOX release for a system with a longer length of the hydrophobic block (i.e. the chain in which DOX was connected). Therefore, it was concluded the designed micelles behaved as expected.

3.4. Cytotoxicity assay

BJ and A549 cell lines, which are human normal fibroblasts and human lung adenocarcinoma cells respectively, were chosen for the *in vitro* cytotoxicity test. The cells were treated with different formulations and the cytotoxic effects were assessed by MTT assay. As seen in Table 3, blank micelles (TPGS-PDMAEMA_m-*b*-PVBA_n) did not show cytotoxic effects on both cell lines at concentrations ranging from 3.9 to 15.6 µg/mL. Low concentrations of the blank micelles (up to 15.6 µg/mL) maintained cell viability at relatively high level (80–95%) compared to the control group. However, by increasing the concentration of bare micelles, the cell viability values decreased, which may be related to the sedimentation of micelles on the cells attached to the bottom of the wells, causing hypoxia effect (deficiency in the amount of oxygen reaching the cells) and mechanical disruption of the cell monolayer, resulting in cell death.

To evaluate the efficacy of the DOX after loading into the micelles, the MTT assay was also performed with free DOX and DOX-conjugated micelles (TPGS-PDMAEMA_m-*b*-PVBA_n-DOX) on both normal and cancer cell lines. The test showed a dose-dependent reduction in the cell viability for all tested samples. In comparison with free DOX with IC₅₀ determined for cancer cells equal to 7.9 µg/mL, two compositions of prepared DOX-conjugated micelles (TPGS-PDMAEMA₁₂₅-*b*-PVBA₃₀-DOX and TPGS-PDMAEMA₁₂₅-*b*-PVBA₉₁-DOX) also showed cytotoxicity effects with IC₅₀ of 5.5 and 8.3 µg/mL, respectively. This indicates slightly higher cytotoxicity towards cancer cells for the DOX-conjugated micelles compared to free DOX. Whereas the third composition showed the highest value of IC₅₀ (21.5 µg/mL) among all tested compounds. Importantly, TPGS-PDMAEMA₁₂₅-*b*-PVBA₃₀-DOX and TPGS-PDMAEMA₁₂₅-*b*-PVBA₉₁-DOX also demonstrated noticeably higher SI values (7.7 and 23.6, respectively) compared to the free DOX (4.6), proving their higher selectivity and thus safety. Therefore, the results revealed that two compositions may be considered as good candidates for drug delivery. All IC₅₀ data and SI were calculated and reported in Table 3.

4. Conclusion

In this study, biocompatible and stimuli-responsive vitamin E-based micelles were developed for the delivery of DOX as a chemotherapeutic agent on the A549 cell line (human lung adenocarcinoma). The designed block copolymers, TPGS-poly(2-(dimethylamino)ethyl methacrylate)-*b*-poly(3-vinyl benzaldehyde), were synthesized by RAFT polymerization. The prepared block copolymers and subsequent micelles were characterized and analyzed by FTIR, ¹H NMR, GPC, DLS, and TEM. The obtained micelles showed high stability as well as drug loading, and encapsulation capacities, which were in the range from 9 to 43%, depending on the copolymer composition. Additionally, *in vitro* cytotoxicity studies exhibited that blank micelles have no significant cytotoxic effects on humans BJ normal cell line. However, DOX-conjugated micelles showed higher cytotoxicity towards the A549 cancer cell line compared to free DOX. Moreover, DOX-conjugated micelles revealed noticeably higher selectivity index compared to the free DOX, proving their higher safety in clinical applications (7.7 and 23.6, for TPGS-PDMAEMA₁₂₅-*b*-PVBA₃₀-DOX and TPGS-PDMAEMA₁₂₅-*b*-PVBA₉₁-DOX, respectively). Because of the presence of vitamin E TPGS on the surface

of prepared micelles, cumulatively, the designed micelles could be considered as good candidates for drug delivery systems, especially for multi-drug resistance cancer therapy.

CRedit authorship contribution statement

Wojciech Raj: Methodology, Validation, Investigation, Writing – original draft. **Krzysztof Jerczynski:** Methodology, Visualization, Investigation, Writing – original draft. **Mahdi Rahimi:** Methodology, Visualization, Writing – original draft. **Ewa Pavlova:** Investigation. **Miroslav Šlouf:** Investigation, Writing – original draft. **Agata Przekora:** Investigation, Writing – original draft. **Joanna Pietrasik:** Conceptualization, Methodology, Writing – review & editing, Supervision.

Declaration of competing interest

The authors declare that they have no known competing financial interests or personal relationships that could have appeared to influence the work reported in this paper.

Acknowledgments

W.R., K.J., M.R., and J.P. acknowledge the financial support from National Science Center, Poland (via Grant UMO-2014/14/A/ST5/00204). Cytotoxicity studies conducted by A.P. were supported by Ministry of Education and Science in Poland within statutory activity of Medical University of Lublin (DS3/2021 project).

Appendix A. Supplementary data

Supplementary data to this article can be found online at <https://doi.org/10.1016/j.polymer.2022.125001>.

References

- [1] R.L. Siegel, K.D. Miller, H.E. Fuchs, A. Jemal, Cancer statistics, 2021, *CA, A Cancer J. Clin.* 71 (1) (2021) 7–33.
- [2] M. Rahimi, V. Shafiei-Irannejad, K.D. Safa, R. Salehi, Multi-branched ionic liquid-chitosan as a smart and biocompatible nano-vehicle for combination chemotherapy with stealth and targeted properties, *Carbohydr. Polym.* 196 (2018) 299–312.
- [3] M. Rahimi, K.D. Safa, R. Salehi, Co-delivery of doxorubicin and methotrexate by dendritic chitosan-g-mPEG as a magnetic nanocarrier for multi-drug delivery in combination chemotherapy, *Polym. Chem.* 8 (47) (2017) 7333–7350.
- [4] V. Shafiei-Irannejad, N. Samadi, R. Salehi, B. Yousefi, M. Rahimi, A. Akbarzadeh, N. Zarghami, Reversion of multidrug resistance by Co-encapsulation of doxorubicin and metformin in poly(lactide-co-glycolide)-d- α -tocopheryl polyethylene glycol 1000 succinate nanoparticles, *Pharmaceut. Res.* 35 (6) (2018) 119.
- [5] G. Zhong, C. Yang, S. Liu, Y. Zheng, W. Lou, J.Y. Teo, C. Bao, W. Cheng, J.P.K. Tan, S. Gao, N. Park, S. Venkataraman, Y. Huang, M.H. Tan, X. Wang, J.L. Hedrick, W. Fan, Y.Y. Yang, Polymers with distinctive anticancer mechanism that kills MDR cancer cells and inhibits tumor metastasis, *Biomaterials* 199 (2019) 76–87.
- [6] L. Kou, R. Sun, Y.D. Bhutia, Q. Yao, R. Chen, Emerging advances in P-glycoprotein inhibitory nanomaterials for drug delivery, *Expert Opin. Drug Deliv.* 15 (9) (2018) 869–879.
- [7] M. Majidinia, M. Mirza-Aghazadeh-Attari, M. Rahimi, A. Mihanfar, A. Karimian, A. Safa, B. Yousefi, Overcoming multidrug resistance in cancer: recent progress in nanotechnology and new horizons, *IUBMB Life* 72 (5) (2020) 855–871.
- [8] N. Majumder, N.G. Das, S.K. Das, Polymeric micelles for anticancer drug delivery, *Ther. Deliv.* 11 (10) (2020) 613–635.
- [9] Z. Gu, C.G. Da Silva, K. Van der Maaden, F. Ossendorp, L.J. Cruz, Liposome-based drug delivery systems in cancer immunotherapy, *Pharmaceutics* 12 (11) (2020) 1054.
- [10] A.B. Cook, S. Perrier, Branched and dendritic polymer architectures: functional nanomaterials for therapeutic delivery, *Adv. Funct. Mater.* 30 (2) (2020) 1901001.
- [11] R. Baghban, M. Afarid, J. Soleymani, M. Rahimi, Were magnetic materials useful in cancer therapy? *Biomed. Pharmacother.* 144 (2021), 112321.
- [12] W. Raj, K. Jerczynski, M. Rahimi, A. Przekora, K. Matyjaszewski, J. Pietrasik, Molecular bottlebrush with pH-responsive cleavable bonds as a unimolecular vehicle for anticancer drug delivery, *Mater. Sci. Eng. C* 130 (2021), 112439.
- [13] F. Masood, Polymeric nanoparticles for targeted drug delivery system for cancer therapy, *Mater. Sci. Eng. C* 60 (2016) 569–578.
- [14] G. Chen, K. Wang, P. Wu, Y. Wang, Z. Zhou, L. Yin, M. Sun, D. Oupický, Development of fluorinated polyplex nanoemulsions for improved small interfering RNA delivery and cancer therapy, *Nano Res.* 11 (7) (2018) 3746–3761.
- [15] I. Ekladios, Y.L. Colson, M.W. Grinstaff, Polymer-drug conjugate therapeutics: advances, insights and prospects, *Nat. Rev. Drug Discov.* 18 (4) (2019) 273–294.
- [16] Q. Zhou, L. Zhang, T. Yang, H. Wu, Stimuli-responsive polymeric micelles for drug delivery and cancer therapy, *Int. J. Nanomed.* 13 (2018) 2921.
- [17] B. Begines, M.V. de-Paz, A. Alcudia, J.A. Galbis, Synthesis of reduction sensitive comb-like polyurethanes using click chemistry, *J. Polym. Sci. Polym. Chem.* 54 (24) (2016) 3888–3900.
- [18] Y. Zhang, Y. Huang, S. Li, Polymeric micelles: nanocarriers for cancer-targeted drug delivery, *AAPS PharmSciTech* 15 (4) (2014) 862–871.
- [19] D. Lombardo, M.A. Kiselev, S. Magazù, P. Calandra, Amphiphiles self-assembly: basic concepts and future perspectives of supramolecular approaches, *Adv. Condens. Matter Phys.* (2015), 151683, 2015.
- [20] Y. Lu, K. Park, Polymeric micelles and alternative nanonized delivery vehicles for poorly soluble drugs, *Int. J. Pharm.* 453 (1) (2013) 198–214.
- [21] H. Jin, J. Pi, Y. Zhao, J. Jiang, T. Li, X. Zeng, P. Yang, C.E. Evans, J. Cai, EGFR-targeting PLGA-PEG nanoparticles as a curcumin delivery system for breast cancer therapy, *Nanoscale* 9 (42) (2017) 16365–16374.
- [22] C. Yang, T. Wu, Y. Qi, Z. Zhang, Recent advances in the application of vitamin E TPGS for drug delivery, *Theranostics* 8 (2) (2018) 464.
- [23] M. Tavares Luiz, L. Delello Di Filippo, R. Carolina Alves, V.H. Sousa Araújo, J. Lobato Duarte, J. Maldonado Marchetti, M. Chorilli, The use of TPGS in drug delivery systems to overcome biological barriers, *Eur. Polym. J.* 142 (2021), 110129.
- [24] Z. Zhang, S. Tan, S.-S. Feng, Vitamin E TPGS as a molecular biomaterial for drug delivery, *Biomaterials* 33 (19) (2012) 4889–4906.
- [25] X. Zhu, A. Tsend-Ayush, Z. Yuan, J. Wen, J. Cai, S. Luo, J. Yao, J. Bian, L. Yin, J. Zhou, Glycyrrhetic acid-modified TPGS polymeric micelles for hepatocellular carcinoma-targeted therapy, *Int. J. Pharm.* 529 (1–2) (2017) 451–464.
- [26] X. Meng, J. Liu, X. Yu, J. Li, X. Lu, T. Shen, Pluronic F127 and D- α -tocopheryl polyethylene glycol succinate (TPGS) mixed micelles for targeting drug delivery across the blood brain barrier, *Sci. Rep.* 7 (1) (2017) 1–12.
- [27] P. Keshari, Y. Sonar, H. Mahajan, Curcumin loaded TPGS micelles for nose to brain drug delivery: in vitro and in vivo studies, *Mater. Technol.* 34 (7) (2019) 423–432.
- [28] J. Chen, A. Ding, Y. Zhou, P. Chen, Y. Xu, W. Nie, Indometacin-loaded micelles based on star-shaped PLLA-TPGS copolymers: effect of arm numbers on drug delivery, *Colloid Polym. Sci.* 297 (10) (2019) 1321–1330.
- [29] X. Zhao, Z. Poon, A.C. Engler, D.K. Bonner, P.T. Hammond, Enhanced stability of polymeric micelles based on postfunctionalized poly(ethylene glycol)-b-poly(γ -propargyl l-glutamate): the substituent effect, *Biomacromolecules* 13 (5) (2012) 1315–1322.
- [30] Y. Dong, P. Du, M. Pei, P. Liu, Design, postpolymerization conjugation and self-assembly of a di-block copolymer-based prodrug for tumor intracellular acid-triggered DOX release, *J. Mater. Chem. B* 7 (37) (2019) 5640–5647.
- [31] A. Przekora, J. Czechowska, D. Pijocha, A. Ślósarczyk, G. Ginalska, Do novel cement-type biomaterials reveal ion reactivity that affects cell viability in vitro? *Open Life Sci.* 9 (3) (2014) 277–289.
- [32] S.S. Ankushrao, Y.S. Patil, V.P. Ubale, N.N. Maldar, A.A. Ghanwat, Synthesis and characterization of thermally stable poly(ether-azomethine)s derived from 1,1-bis[4-(4-benzaldehyde oxy)-3-methyl phenyl] cyclopentane, *J. Macromol. Sci., Part A* 54 (6) (2017) 411–417.
- [33] S. Tu, Y.W. Chen, Y.B. Qiu, K. Zhu, X.L. Luo, Enhancement of cellular uptake and antitumor efficiencies of micelles with phosphorylcholine, *Macromol. Biosci.* 11 (10) (2011) 1416–1425.
- [34] L. Deng, G. Wang, J. Ren, B. Zhang, J. Yan, W. Li, N.M. Khashab, Enzymatically triggered multifunctional delivery system based on hyaluronic acid micelles, *RSC Adv.* 2 (33) (2012) 12909–12914.
- [35] Y. Jiang, Y. Zhou, C.Y. Zhang, T. Fang, Co-delivery of paclitaxel and doxorubicin by pH-responsive prodrug micelles for cancer therapy, *Int. J. Nanomed.* 15 (2020) 3319.
- [36] Y. Mi, J. Zhao, S.-S. Feng, Vitamin E TPGS prodrug micelles for hydrophilic drug delivery with neuroprotective effects, *Int. J. Pharm.* 438 (1) (2012) 98–106.